Surface Photovoltage of Porphyrin Layers Using the Kelvin Probe Technique

Ellen Moons* and Albert Goossens

Laboratory of Applied Inorganic Chemistry, Delft University of Technology, Julianalaan 136, 2628-BL Delft, The Netherlands

Tom Savenije

Laboratory of Molecular Physics, Wageningen Agricultural University, Dreyenlaan 3, Wageningen, The Netherlands

Received: March 25, 1997; In Final Form: May 30, 1997[⊗]

The Fermi energy of spin-coated layers of pyridinium porphyrins on indium tin oxide (ITO) was determined by the Kelvin probe technique. The work function of zinc tetrakis(*N*-methyl-4-pyridinium)porphyrin (ZnTMPyP) was found to be 500 meV larger than the one of metal-free tetrakis(*N*-methyl-4-pyridinium)-porphyrin (H_2TMPyP), which indicates that the Fermi levels ascribed to these molecular layers do not lie in the middle of their energy gap but that the layers show a p-type and an n-type character, respectively. Furthermore, from the dependence of the work function on the layer thickness, we deduce that an electric field is present near the porphyrin/ITO interface. This field extends over 10−20 nm and is oriented such that the porphyrin layers are depleted from majority mobile carriers near the ITO interface. However, this field does not contribute significantly to the photovoltage, which indicates a high density of interface traps at the ITO interface. Surface photovoltage measurements under illumination of the porphyrin molecules indicate that an additional depletion region is present at the porphyrin/air interface. We therefore suggest for the porphyrin/ITO system a double junction model. This double junction was simulated numerically and values for the surface charge density and the interface charge density were extracted.

Introduction

Solid molecular layers receive a lot of attention as promising constituents in (opto)electronic devices and sensors. The wide selection of organic molecules and their flexibility in deposition and modification in accordance with desired physical properties give them advantages above the conventional building blocks of semiconductor electronics. For the use in thin film organic solar cells, pigments with a high absorption coefficient in the visible range receive special interest. Particularly the analogues of the natural chlorophyll pigments, such as porphyrins and phthalocyanines, are components of first choice for the construction of an artificial photosynthetic system.[1,2] Phthalocyanines and porphyrins have been used in single-dye Schottky barrier type devices[3−5] and phthalocyanines in particular also as hole conductors (p-type layers) in heterojunction devices.[6−9] Photoinduced charge separation has been reported in heterojunctions between an organic electron-conducting layer and an organic hole conductor. A systematic study on the device structure was published by Whitlock et al.[10] These dyes have also been applied as photosensitizers of large bandgap oxidic semiconductors, such as TiO_2.[11−15] Crucial questions in the field of organic devices, and p/n junctions in particular, are the following: (1) Does a certain molecular layer act as an n-type or p-type semiconductor? (2) Where are the electric fields that are responsible for the rectifying behavior and for the photovoltaic behavior situated? In other words, are the contacts with the electrodes ohmic? Is there an electric field at the interface between two molecular layers? (3) Is the interfacial electric field between the two organic layers extended over a certain width as a space charge layer or is it located within a few monolayers from the interface as an interfacial dipole?

Due to the high position of the energy levels of most porphyrins, very few of them have n-type like behavior. For a molecule in solution, electron-withdrawing substituents cause the molecular orbital levels to shift to lower energy and electron-donating substituents shift the energy levels to higher energy. It was reported that the "band edges" of thin solid films of these compounds shift in the same way.[16,17]

Heterojunctions consisting of two different porphyrins have been studied as potential photocells.[18,19] Rectification and photovoltaic behavior have been reported and open circuit voltages of 0.4 eV are achieved for the Hg/H_2TMPyP/Zn-tetrakis(hydroxyphenyl)porphyrin (ZnTHOPP)/ITO heterojunction. The purpose of this work is to shed light on the above-mentioned problems of the heterojunction by studying the electrical properties of the interfaces of the individual layers of two pyridinium porphyrins with the ITO electrode. The formation of a Schottky barrier type junction in a zinc tetraphenylporphyrin layer (ZnTPP) in contact with a metal has previously been demonstrated by impedance measurements[20,21] and by UV-photoemission spectroscopy (UPS).[22] The Kelvin probe technique is an established direct, noncontact method in semiconductor surface electronics[23] to determine the work function of a (semi)conducting solid. The technique has also been proven useful for the determination of the surface potential of monolayers of organic molecules (L−B layers, self-assembled layers) on solid substrates[24,25] and to evaluate the effect of adsorbates on the work function of semiconductors.[26−28] Additionally, surface photovoltage measurements (SPV) and surface photovoltage spectroscopy (SPS) can be carried out using the Kelvin probe technique and yield information about the band bending near the surface of a semiconductor[29] and/or the built-in voltage at the buried interface inside a heterojunction.[30,31] SPS can provide information about the energetic position of localized levels inside the bandgap.[32] We report

* Corresponding author. Present address: Lab. Photonique et Interfaces, EPFL, CH-1015 Lausanne, Switzerland.

[⊗] Abstract published in *Advance ACS Abstracts,* October 1, 1997.

S1089-5647(97)01071-7 CCC: $14.00

here on the use of the Kelvin probe technique to determine the position of the Fermi level of extended molecular layers and to evaluate the electric fields present in organic/inorganic hybrid structures. The Fermi energy of the organic constituents of electronic devices is an essential parameter for the understanding and optimization of device performance. Band edge positions of various molecular solids, among which are phthalocyanine layers, were determined by UPS measurements.[16,21,33] However, by this technique the position of the Fermi level of the organic layer cannot be determined and observed positions of the band edges are relative to the Fermi level of the metal substrate. In recent studies, the effect of doping of organic pigment films on the position of the Fermi level was investigated by the Kelvin probe method e.g. for zinc phthalocyanine (ZnPc) with perfluorinated ZnPc[34] and for perylenes.[35]

We selected two tetrakis(*N*-methyl-4-pyridinium)porphyrins with a different central substituent (Zn or 2 H) with the purpose of studying the effect of the central substituent on the work function and the conduction type of the porphyrin layer. The meaning of Fermi level and work function of a molecular solid are discussed critically. Further, we applied SPV and SPS methods to estimate the electric fields near the surface and buried at the organic/inorganic interface.

Experimental Section

Free base tetrakis(methylpyridinium)porphyrin (H_2TMPyP) and zinc tetra(*N*-methyl-4-pyridinium)porphyrin (ZnTMPyP) (Strem Chemicals, Posen, IL) layers were made by spin coating solutions of the corresponding chlorides in methanol at 3000 rpm on ITO substrates (Glastron). Layers of various thicknesses were made by changing the concentration of the solution between 2 mM and 0.3 μM. The samples were heated for 30 min in air at 100 °C, stored in sealed vessels, and kept in the dark. The thicknesses of the layers were determined by measuring the optical absorbance and were corrected for reflection using a diffuse reflectance sphere (Cary 5e, Varian). Using a step-profilometer the absorbance could be correlated to the thickness of the organic layer.[36]

No crystal growth could be detected in the layers by optical microscopy. The morphology of the spin-coated layers has been investigated by atomic force microscopy. The porphyrin layers of several tens of nanometers thickness on ITO could not be distinguished from those of bare ITO. From this and from the broadening of the peaks in the UV/vis absorption spectra of the porphyrin layers with respect to the spectra of the corresponding porphyrin in solution, which indicates an inhomogeneity of the layer, we conclude that the spin-coated layers are amorphous. On the basis of the fact that current/voltage characteristics of the layers could be recorded with a Hg drop as top contact,[19] we are assured that the layers are free of pinholes.

Contact potential difference (CPD) measurements were carried out using a DC electrostatic voltmeter (Trek 320B) with a high-sensitivity probe (model 3250). The Kelvin probe technique is a noncontact method to measure the potential between a reference probe and a sample surface that have been brought in close proximity of each other (distance about 1 mm).[37−39] By electromechanically vibrating the reference probe with respect to the sample surface, which is back-contacted and grounded, an ac current appears in the external circuit due to the modulation of the capacitance in the presence of an electrostatic field. By a phase-sensing demodulator and a feedback loop, the amplitude of this current is nulled. The externally applied voltage that is needed to null the current is the actual readout of the measurement and is equal but opposite in sign to the CPD. The work function of the sample can then be calculated from the CPD by subtracting the measured value for the CPD from the work function of the metal reference probe, which is assumed to be constant. Here we take 5.1 ± 0.1 eV as the work function of the reference probe, a value that was obtained after calibration with respect to a sputtered layer of Au on glass and ITO and with Pt metal. The CPD can be determined with an accuracy of 10 mV. The error on absolute values for the work function is much larger and depends mainly on noise and on the reliability of the work function of the reference probe.[40,41]

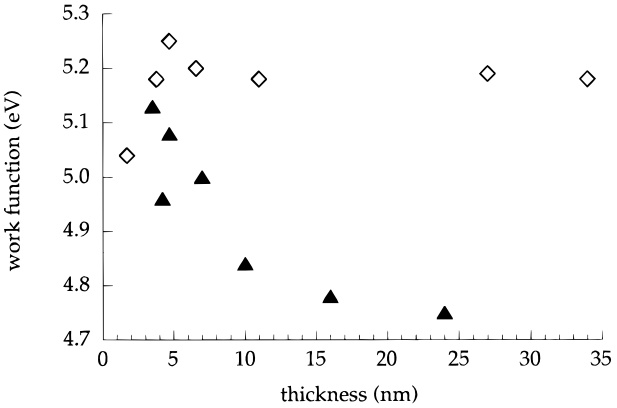

Figure 1. Dependence of the work function, Φ (eV), of ZnTMPyP (◇) and H_2TMPyP (▲) layers on the layer thickness.

The surface photovoltage is the change of the work function of the sample upon illumination. The samples are illuminated through the transparent substrate side by light from a Xe lamp (450 W) with wavelength selection by a monochromator (Oriel 1/8m). The white light intensity was about 1 W/m^2, as determined using a power meter (Kipp & Zonen). Wide monochromator slits ($\Delta\lambda \approx 10$ nm) were used. Care was taken that the light was focused on the sample area under the reference probe (diameter about 5 mm).

The SPV spectra are obtained by scanning the wavelength of the incident light through the visible and UV range (850−300 nm) with a rate of 25 nm/min. The photovoltage signal is fed into a computer via an A/D converter. Cutoff filters (Schott GG495, WG305) were exchanged during the measurement. The SPV spectra have not been corrected for the spectrum of the Xe lamp. For the "double-beam" experiments, an additional halogen lamp (Schott) equipped with two cutoff filters (Schott WG345 and GG395) was used.

Results

By CPD measurements in the dark, the work functions of solid layers of ZnTMPyP and H_2TMPyP on ITO substrates were determined. In order to determine whether or not there is an electric field in the layer, and if there is, where it is located, a series of films with increasing thickness was measured.

The work function of a 25 nm thick layer of ZnTMPyP on ITO is 5.20 ± 0.05 eV. This is substantially larger than the work function for a H_2TMPyP layer of the same thickness on ITO, which is 4.75 ± 0.05 eV. For the work function of H_2TMPyP layers on SnO_2 and for ZnTMPyP layers on TiO_2, similar values were found, confirming that the work function of these layers does not depend on the substrate.

The results show that the work function depends on the thickness of the porphyrin layer, Figure 1. The work function evolves from 5.05 ± 0.03 eV, i.e., a value close to that for ITO, for the thin layers of both porphyrins to higher values for thicker layers of ZnTMPyP and to lower values of thicker layers

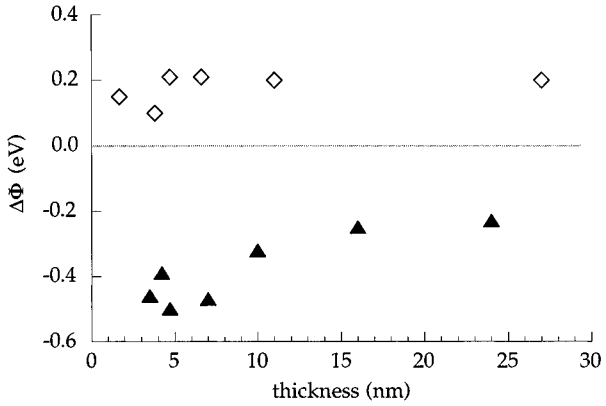

Figure 2. Dependence of the change in work function, $\Delta\Phi$ (eV), of H_2TMPyP (▲) and ZnTMPyP (◇) layers due to illumination with 440 nm light on the layer thickness.

of H_2TMPyP. This dependence yields the potential distribution in the layer. At low thicknesses effects of less than perfect coverage can not be excluded.

In Figure 2, the change of the work function upon illumination at 440 nm (the porphyrin Soret band) through the ITO substrate is shown as a function of the layer thickness. For ZnTMPyP, the work function increases upon illumination, while it decreases for H_2TMPyP. The overall increase is about 0.2 eV, and this value is obtained for layers thicker than 7 nm; the decrease saturates at about 0.2 eV for a layer thickness of about 25 nm. Surprisingly, thinner layers of H_2TMPyP show larger photovoltages, which is probably caused by an independent subbandgap response of the ITO.

The question arises whether or not the light can pass through the whole porphyrin layer without being totally absorbed. From optical transmission measurements it appears that only 64% of the 440 nm light is absorbed by a 25 nm layer of H_2TMPyP.

The SPV spectra, Figure 3, consist of two parts: the band-to-band transition near the bandgap energy of ITO at about 350 nm and the porphyrin absorption in the visible region. The visible region of the SPV spectrum is similar to the optical absorption spectrum of the porphyrin, though the spectral dependence is much weaker. The photovoltage signal starts at about 650 nm, corresponding to the high wavelength peak in the absorption spectrum of the used porphyrins. The photovoltage does not change much upon scanning toward lower wavelengths, indicating that excitation even at 650 nm generates enough photoelectrons to approach saturation, i.e., annihilation of the internal field. This implies that the light intensity at 440 nm (20 times more absorption) is probably high enough to reach the "flat band" situation.

The base line of the spectra is offset from zero with an amount equal to the contact potential difference in the dark. The shape of the spectrum changes with the layer thickness. The thicker the porphyrin layer, the larger the part of the spectrum that is due to porphyrin absorption. Saturation is reached for both porphyrins at layer thicknesses between 10 and 20 nm.

The SPV spectrum of bare ITO shows an absorbance that starts even at subbandgap energy corresponding to about 550 nm. Bare ITO shows a photovoltage of about 500 mV at the bandgap energy ($E_g = 3.7-4.3$ eV[42,43]). SPV spectra of thin layers of each porphyrin show a relatively large response at ITO bandgap energy.

To verify the presence of a depletion layer in the ITO, we carried out so-called "double-beam" Kelvin probe measurements using 325 nm excitation light of a Xe lamp and of a halogen light source with UV filter (transmitting $\lambda > 345$ nm). The purpose of this experiment is to measure the band bending in

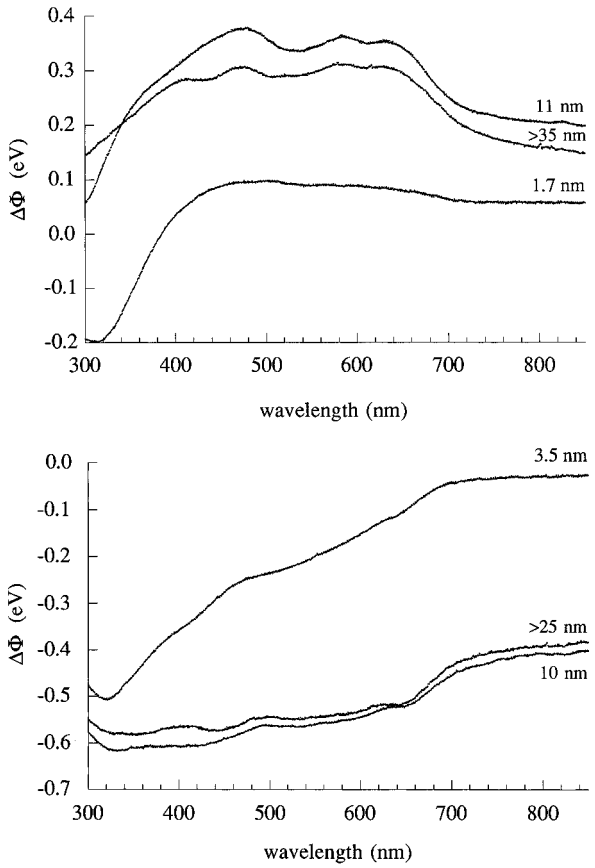

Figure 3. SPV spectra of layers of (a) ZnTMPyP and (b) H_2TMPyP with various thicknesses. The spectra were not normalized, meaning that they are shifted with respect to each other with a value corresponding to the change in the work function measured in the dark.

the ITO while the porphyrin is excited. Under these conditions, we do not expect the light from the Xe lamp to influence significantly the position of the Fermi level of the porphyrin, because the latter is close to the flat band position. However, a change in the photovoltage upon illumination with 325 nm light was observed, which indicates that the ITO is still slightly depleted and that the injection of electrons from excited porphyrins is not sufficient to flatten the bands of the ITO completely. For the 25 nm thick H_2TMPyP layer, the photovoltage upon illumination with 325 nm light is up to 30 meV, while for the thickest ZnTMPyP/ITO layer it was up to 90 meV. Therefore, the corrected value for the photovoltage of H_2TMPyP is 170 mV (ITO response to light yields photovoltage in the same direction as H_2TMPyP response), while for ZnTMPyP, the corrected value is 290 mV (ITO response in the opposite direction as ZnTMPyP). These results assure us that the ITO is depleted when contacted with either of the porphyrin layers.

Discussion

Fermi level. To describe the energetic properties of molecular semiconductors, we will use two different models as guidelines: the inorganic semiconductor model and the molecular one.

In classical semiconductors, long range order and significant orbital overlap cause the creation of energy bands that are separated from each other by a forbidden gap. The Fermi level is then defined as the energy at which the probability of finding an electron is one-half, and this level usually lies in the bandgap between the top of the valence band and the bottom of the conduction band. The Fermi level is also the electrochemical potential for electrons. Molecular solids are mainly used in

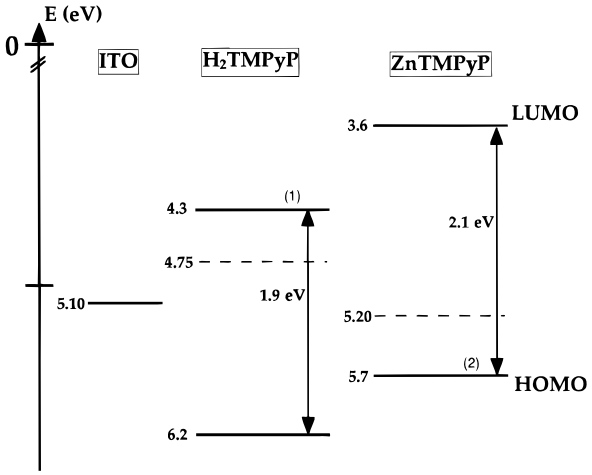

Figure 4. Energy diagram showing the measured work functions and the positions of the band edges ((1) and (2) were taken from refs 22 and 47 of ZnTMPyP and H_2TMPyP layers.

amorphous form for device applications and do not have long range order as semiconductors have. The formation of well-defined energy bands is therefore questionable.

For molecules, the energy levels are discrete. The energy of the electron-accepting species of the molecule is the energy of the oxidized state, which is higher than that of the electron-donating species, the reduced state. For such a system, the electrochemical potential of the electrons, $\bar{\mu}$, corresponds to the Fermi level for a solid. According to Gerisher,[44] the Fermi level, as defined above, is equivalent to the redox potential, except for the reference level. Despite the heavy dispute about this topic in the literature,[45] it can be demonstrated[46] that the Fermi level can serve as a redox potential. For a molecule in its ground state, the electron of highest energy defines the HOMO (highest occupied molecular orbital) level. Upon electronical excitation, the energetically lowest state defines the LUMO (lowest unoccupied molecular orbital) level.

For molecular solids, both above-described models are used. We have chosen to base our discussion of the experimental results on the semiconductor band model[4,8,20,21] and to use semiconductor terminology to describe their electronic properties. This is acceptable, if we keep in mind that the porphyrin layers are not electronic semiconductors, but rather insulating layers with low charge carrier mobility. We prefer, however, to use the terms HOMO and LUMO instead of the valence band maximum and the conduction band minimum. The positions of the HOMO and LUMO levels of solid layers versus the vacuum level can be identified with the ionization potential and electron affinity, respectively, as measured by photoemission. The applicability of this model to the porphyrin system was discussed previously.[19]

From the Kelvin probe measurements we obtain directly the position of the Fermi level of the electrons in the molecular solid with respect to the vacuum level. We have observed that the Fermi level of ZnTMPyP lies lower in energy than the Fermi level of H_2TMPyP. This is in agreement with the relative positions of the reduction potential of ZnTMPyP and the oxidation potential of H_2TMPyP in solution. As shown in Figure 4, the Fermi level of the solid ZnTMPyP layer lies close to this molecule's oxidation level (5.7 eV vs vacuum) and the one of the solid H_2TMPyP layer close to the reduction level of H_2TMPyP in solution (4.3 eV vs vacuum).[47] However, the oxidation and the reduction level of the ZnTMPyP molecule are both higher in energy than the respective levels of H_2TMPyP.

The HOMO−LUMO gaps, shown in Figure 4, were deduced from the long wavelength absorption band at 600 nm for ZnTMPyP and at 650 nm for H_2TMPyP in the optical absorption spectra of the solid layers. For the positions of the LUMO level of H_2TMPyP and the HOMO level of ZnTMPyP represented in Figure 4, the reduction and oxidation potentials[47] were taken, respectively. Direct measurements of the positions of the HOMO and LUMO levels of solid porphyrin and phthalocyanine layers by photoemission have been reported earlier.[16,22]

From this we conclude that the Fermi levels of the solid porphyrin layers do not lie halfway between the HOMO and the LUMO level, but the Fermi level of ZnTMPyP lies closer to the HOMO level, while that of H_2TMPyP lies closer to the LUMO level. Considering the analogy with semiconductor electronics, ZnTMPyP is called a p-type material and H_2TMPyP an n-type. A similar correlation between the energy level positions and the conduction type is reported for other porphyrins[22] and for phthalocyanines.[16] It is worthwhile to point out that the effect we observe cannot be a simple consequence of charging of an insulating layer in the electric field under the probe because that cannot explain the difference between the values for ZnTMPyP and H_2TMPyP.

The thickness dependence of the measured work function shows that an electric field is present in the layer near the interface with the ITO. It extends over a thickness of less than 5 nm for ZnTMPyP and more than 20 nm for H_2TMPyP. The fact that the space charge region is wider for H_2TMPyP than for ZnTMPyP indicates a higher majority carrier density in the ZnTMPyP (holes) than in the H_2TMPyP (electrons),[24] probably due to a larger defect concentration.

The field near the ITO interface is directed such as to create a depletion region for both porphyrin layers, i.e., a downward band bending for the p-type ZnTMPyP and an upward bending for the n-type H_2TMPyP. Because ITO is a degenerate semiconductor and behaves like a metal, the formation of such a depletion region is analogous to the formation of a Schottky barrier between a metal and a semiconductor. In other words, when ZnTMPyP (measured work function 5.2 eV) is brought in contact with ITO (measured work function 5.0 ± 0.1 eV), a p-type depletion region will be formed in the ZnTMPyP layer. Analogous arguments can be applied to explain the n-type depletion region in the H_2TMPyP layer at the ITO interface. For the porphyrins used in this work, the Schottky model can explain the presence of the interfacial field. The question arises whether such an interfacial electric field is sufficient to explain the photovoltaic behavior of these layers and of the acceptor/donor/ITO solar cell, built up from such porphyrin layers.

Illumination. Upon illumination of an inorganic semiconductor, mobile carriers are generated that separate and compensate the electric field present in the layer or recombine. If they compensate the field, we will observe a shift of the Fermi level upon illumination, which is equal to the photovoltage. If the light intensity is high enough to annihilate the field completely, the flat band situation is reached and the saturation value of the photovoltage is then indicative for the band bending that is present in the layer in the dark. If the carriers recombine in surface states or bulk states, they do not induce any shift of the Fermi level and therefore they do not contribute to the photovoltage. The mechanism of photocurrent generation in molecular semiconductors is usually described by means of exciton generation, diffusion, and dissociation into charge carriers. These mobile charge carriers will accelerate in opposite directions, if an electric field is present, and hence annihilate the electric field in a similar way as in an inorganic semiconductor.

Upon illumination of the porphyrin layers with visible light, the direction of the change in work function is opposite to what

we would expect, if there were only an electric field near the ITO interface and this one were annihilated upon illumination. In other words, it appears that additional fields are present in the layer. The sign of this photovoltage for ZnTMPyP and H_2-TMPyP correlates with the behavior of a surface depletion in a p-type and n-type semiconductor, respectively, under illumination. Therefore, we conclude from the sign of the photovoltage that an electric field is present at the air/porphyrin surface, whose direction is opposite to the field near the ITO.

Such a surface depletion layer is not evident from the results of the dark work function measurements. The position of the Fermi level measured in the dark is determined by the overall field present in the layer. The observation that the work function of the ZnTMPyP layer is larger than the work function of bare ITO only means that the interface band bending (which increases the measured work function) must be larger than the surface band bending (which lowers the measured work function). Analogously, also for H_2TMPyP, the interface band bending must be larger than the surface band bending. However, apparently it is dominantly the surface field which contributes to the photovoltage. There are several possible reasons why the interface field is less photoactive: (1) the excitons do not dissociate at the interface but are reflected or undergo radiative or nonradiative decay or (2) the excitons dissociate at the interface, but the mobile carriers recombine immediately. An indication that the porphyrin/ITO interface has a high density of recombination centers is obtained from the double-beam experiments.

The SPV spectrum of bare ITO shows an absorbance that starts at subbandgap energy corresponding to about 550 nm and a photovoltage of about 500 mV at the bandgap energy. Also the SPV spectra of thin layers of both porphyrins show a relatively large response at ITO bandgap energy. This subbandgap photovoltage could possibly be due to the excitation of electrons from acceptor surface states in the forbidden gap about 2.3 eV under the conduction band, to the conduction band. However, ITO has a weakly absorbing indirect bandgap at 2.8 eV (443 nm), and in the subbandgap region an Urbach tail is present that can stretch from 2.8 to 2.3 eV (550 nm).[42,48,49] We interpret the large photovoltage in bare ITO as due to the band-to-band transition in the ITO, indicating the presence of a depletion layer. The thicker the porphyrin layers, the smaller the band bending in ITO. It is difficult to extract quantitative information about the band bending in ITO from these measurements, because the signal at 350 nm is not purely caused by ITO. The measured is a sum of the change of the ITO work function and the photoinduced change in the porphyrin layer (which goes in the opposite direction in the case of ZnTMPyP and in the same direction in the case of H_2TMPyP). Since the optical absorption spectra of porphyrin and ITO have some overlap, i.e., the porphyrin also absorbs in the UV region, the interpretation of the results is complicated. This overlap also disturbs the measurements at 440 nm of thin porphyrin layers, mentioned above, where ITO still absorbs.

Double-Junction Model. To explain the $I-V$ behavior as well as the photovoltage response of the Hg/H_2TMPyP/ITO junction, an electrostatic junction model has been elaborated. For the ZnTMPyP/ITO case an analogous reasoning could be put forward. This model considers a highly conducting (degenerate) semiconductor substrate (such as ITO substrates) onto which insulating (organic) films are applied. The organic films are regarded as being fully depleted in the sense that all the free electrons are removed leading to a uniform and positive space charge density, ρ_F. At the air/film interface a negative surface charge density, σ_s, is present, and at the film/substrate

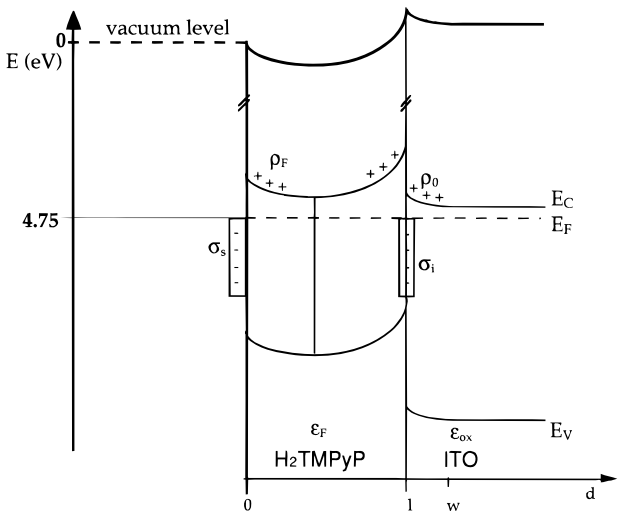

Figure 5. Energy diagram of the H_2TMPyP/ITO structure. Symbols are defined in the text.

interface an additional negative interface charge density, σ_i, exists. Since the organic film, together with the interface charges and the substrate space charge, fulfill electrical neutrality, the space charge in the ITO substrate, ρ_{ox}, balances the other charges. Accordingly, the situation as drawn schematically in Figure 5 is considered.

To calculate the internal potential distribution, Gauss's law is applied, i.e.

$$E(x) = \frac{Q(x)}{\epsilon_F \epsilon_0 A} \tag{1}$$

where $Q(x)$ is the total charge enclosed inside a Gaussian box with wall coordinates 0 and x. ϵ_0 is the permitivity of free space. A is the surface area. The dielectric constant of the film, ϵ_F, is included to allow for electrostatic screening. Since the space charge inside the film is uniform, for $x < l$, l being the film thickness

$$Q(x) = \sigma_s A + \rho_F A x \tag{2}$$

By using the definition of the potential, i.e.

$$\varphi(x) = -\int_0^x E(\xi)\, \mathrm{d}\xi \tag{3}$$

we write

$$\varphi(x) = -\frac{1}{\epsilon_F \epsilon_0}\left(\sigma_s x + \frac{1}{2}\rho_F x^2\right) \tag{4}$$

The zero potential, $\varphi(x{=}0) = 0$, was chosen at the film/air interface, where the Kelvin probe measurement takes place. As follows immediately from eq 4, inside the film there is a plane at which $E = 0$ and where the potential reaches a local minimum. This plane is found at $x = -\sigma_s/\rho_F$, and the local potential minimum, φ_{min}, there is

$$\varphi_{min} = \frac{\sigma_s^2}{2\epsilon_F \epsilon_0 \rho_F} \tag{5}$$

At $x > l$, the enclosed charge in the Gaussian box reads

$$Q(x) = \sigma_s A + \rho_F A l + \sigma_i A + \rho_{ox}(x - l)A \tag{6}$$

and the local electric field is given by

$$E(x) = \frac{1}{\epsilon_F \epsilon_0}(\sigma_s + \rho_F l + \sigma_i + \gamma \rho_{ox}(x - l)) \quad (7)$$

where $\gamma = \epsilon_F/\epsilon_{ox}$, ϵ_{ox} being the dielectric constant of ITO. The potential inside the ITO substrate is given by

$$\varphi(x) = -\int_l^x E(\xi)\, d\xi + \varphi(l) \quad (8)$$

being

$$\varphi(x) = \frac{-1}{\epsilon_F \epsilon_0}\left(\frac{1}{2}\gamma \rho_{ox} x^2 + \{\sigma_s + \sigma_i + (\rho_F - \gamma \rho_{ox})l\}x - \sigma_i l - \frac{1}{2}(\rho_F - \gamma \rho_{ox})l^2\right) \quad (9)$$

At the film/ITO interface, i.e. $x = l$, the potential equals

$$\varphi(l) = \frac{-1}{\epsilon_F \epsilon_0}\left(\sigma_s l + \frac{1}{2}\rho_F l^2\right) \quad (10)$$

At $x = l + w$ is a plane in the ITO where the field is zero and the potential reaches a characteristic value. This is the edge of the depletion region, and the potential at this edge is equal to the potential inside the neutral ITO bulk region. Using eq 7 one finds

$$l + w = \frac{-1}{\gamma \rho_{ox}}(\sigma_s + \sigma_i + (\rho_F - \gamma \rho_{ox})l) \quad (11)$$

and the potential of the ITO bulk region, i.e., $x \geq l + w$, is given by

$$\varphi(l + w) = \frac{1}{\epsilon_F \epsilon_0}\left(\frac{1}{2\gamma \rho_{ox}}\{\sigma_s + \sigma_i + (\rho_f - \gamma \rho_{ox})l\}^2 + \sigma_i l + \frac{1}{2}(\rho_F - \gamma \rho_{ox})l^2\right) \quad (12)$$

It is this potential that is measured with the Kelvin probe in the dark. Upon irradiation, the equilibrium potential distribution changes and the bands are flattened. With SPV three potential drops can, in principle, be measured. The first is the potential drop at the film/air interface, i.e., φ_{min}, the second is the potential drop in the film at the film/ITO interface, i.e., $\varphi(l) - \varphi_{min}$, and the third is the potential drop inside the ITO, i.e., $\varphi(l+w) - \varphi(l)$.

The SPV results are interpreted as follows. Upon excitation of the organic film, excitons are generated. Excitons diffuse through the film, some to the film/air surface, others to the film/ITO interface. The question arises, what happens to these excitons when they reach the surface of interface—will they dissociate into electron−hole pairs or not? Only if they do dissociate and the generated mobile carriers separate can a photovoltage be produced. We postulate that at the film/air surface the excitons dissociate and electrons and holes are separated. The hole will be trapped in one of the many negatively charged surface states. The electron escapes to the inside of the film, accelerated by the local electric field. Electrons are thus accumulated inside the film, leading to a photovoltage. As soon as the flat band situation is established, the driving force for electron drift has vanished and the built up photovoltage equals the band bending.

In contrast, when an exciton arrives at the film/ITO interface, charge separation does not take place. There are two possibilities: (1) the excitons do not dissociate at the interface but are reflected or undergo radiative or nonradiative decay, or (2) the excitons dissociate at the interface but the mobile carriers recombine immediately. Our technique is not able to distinguish between these different scenarios.

Upon irradiation of the porphyrin film, a photovoltage is obtained given by

$$\Delta\varphi = \varphi_{min} = \frac{\sigma_s^2}{2\epsilon_F \epsilon_0 \rho_F} \quad (13)$$

We consider here only the case where the interface does not contribute to the photovoltage. For ϵ_F, a value between 3 and 5 is expected in the case of most porphyrin/phthalocyanine-based organic films.[19] The measured space charge region width of about 5 nm for ZnTMPyP and about 20 nm for H_2TMPyP can be used to derive a value for ρ_F. For a semiconductor with donor density, N_D, the space charge region width is given by

$$W = W_0 U^{1/2} = \sqrt{\frac{2\epsilon_F \epsilon_0}{eN_D}}\, U^{1/2} \quad (14)$$

where U is the band bending. For H_2TMPyP and ZnTMPyP, a photovoltage, i.e., a band bending, of 0.2−0.3 V is measured. Upon substitution into eq 14 we find for the donor concentration for H_2TMPyP, $N_D = 3.5 \times 10^{17}$ cm^{-3}, and for the acceptor concentration for ZnTMPyP, $N_A = 5.5 \times 10^{18}$ cm^{-3}. Then the space charge densities in the films are $\rho_F = N_D \cdot e = 5.6 \times 10^4$ C m^{-3} for H_2TMPyP and $\rho_F = N_A \cdot e = -8.9 \times 10^5$ C m^{-3} for ZnTMPyP. From these values the surface charge densities, σ_s, can be derived. Using $\varphi_{min} = U = 0.25$ V and $\epsilon_F = 5$ for both films, we find for H_2TMPyP, $\sigma_s = -1.1 \times 10^{-3}$ C m^{-2}, i.e., monovalent surface state density $= 6.9 \times 10^{15}$ m^{-2}, and for ZnTMPyP, $\sigma_s = +4.4 \times 10^{-3}$ C m^{-2}, i.e., monovalent surface state density $= 2.8 \times 10^{16}$ m^{-2}.

When the ITO support is excited, the bands in the ITO at the film/ITO interface flatten and the photovoltage in that case reads

$$\Delta\varphi_{ITO} = \varphi(l+w) - \varphi(l) = \frac{1}{\epsilon_F \epsilon_0}\left\{\frac{1}{2\gamma \rho_{ox}}[\sigma_s + \sigma_i + (\rho_F - \gamma \rho_{ox})l]^2 + (\sigma_s + \sigma_i)l + \left(\rho_F - \frac{1}{2}\gamma \rho_{ox}\right)l^2\right\} \quad (15)$$

Equation 15 can be rewritten as

$$\sigma_i^2 + A\sigma_i + B = 0 \quad (16)$$

with

$$A = 2(\sigma_s + \rho_F l)$$

$$B = (\sigma_s + \rho_F l)^2 - 2\epsilon_F \epsilon_0 \gamma \rho_{ox} \Delta\varphi_{ITO}$$

The solutions σ_i of the quadratic equation are then

$$\sigma_i = -(\sigma_s + \rho_F l) \pm \sqrt{2\epsilon_F \epsilon_0 \gamma \rho_{ox} \varphi_{ITO}} \quad (17)$$

For the H_2TMPyP/ITO structure the band bending in ITO is $\Delta\varphi_{ITO} = 0.03$ V, and for the ZnTMPyP/ITO structure $\Delta\varphi_{ITO} = 0.09$ V. Substituting these values and $\epsilon_{ox} = 8.9$, $\epsilon_F = 5$, $\rho_{ox} = e \times 10^{26}$ m^{-3} $= 1.6 \times 10^7$ C m^{-3}, and the above calculated values for σ_s and ρ_F into eq 17, we can derive a value for σ_i. For H_2TMPyP, $\sigma_i = 5.7 \times 10^{-3}$ C m^{-2}, i.e. monovalent interface state density $= 3.2 \times 10^{16}$ m^{-2}, and for ZnTMPyP there are two possible solutions: $\sigma_i = +2.6 \times 10^{-2}$ C m^{-2} or $\sigma_i = +9.3 \times 10^{-3}$ C m^{-2}. From the charge neutrality equation

$$\sigma_s + \rho_F l + \sigma_i + \rho_{ox} w = 0 \quad (18)$$

with $w = 9.4 \times 10^{-10}$ m, the space charge width in ITO, we find that $\sigma_i = +2.6 \times 10^{-2}$ C m^{-2} is the correct solution of the quadratic equation for ZnTMPyP. The monovalent interface state density is then 1.6×10^{17} m^{-2}.

Conclusions

The work functions of two different pyridinium porphyrin layers on ITO were determined by the Kelvin probe technique. The ZnTMPyP has a work function that is 500 meV higher than the H_2TMPyP. These results indicate that the Fermi level that can be ascribed to this molecular layer does not lie in the middle between the oxidation and reduction level of the molecule, as is often assumed, but that the layers show a p-type and n-type character, respectively.

From the distance dependence of the work function measured in the dark, we conclude that there is a field present at the interface. This field is such that the porphyrin layers are depleted at the ITO interface.

The direction of the photovoltage upon illumination of the porphyrin indicates that also a surface field with opposite direction is present in the dark. We interpret this as the presence of an additional depletion region at the porphyrin/air interface, with a smaller band bending than the one at the porphyrin/ITO interface. For the H_2TMPyP/ITO system the double-junction model is presented in Figure 5. By numerical simulation a surface state density of 6.9×10^{15} m^{-2} for H_2TMPyP and 2.8×10^{16} m^{-2} for ZnTMPyP and an interface state density of 3.2×10^{16} m^{-2} for H_2TMPyP and 1.6×10^{17} m^{-2} for ZnTMPyP are found.

References and Notes

(1) Wöhrle, D.; Meissner, D. *Adv. Mater.* **1991**, *3*, 129−138.
(2) Savenije, T. J. Ph.D. Thesis, Wageningen Agricultural University, 1997.
(3) Siebentritt, S.; Gunster, S.; Meissner, D. *Synth. Met.* **1991**, *41*−*43*, 1173−1176.
(4) Harima, Y.; Yamamoto, K.; Takeda, K.; Yamashita, K. *Bull. Chem. Soc. Jpn.* **1989**, *62*, 1458−1462.
(5) Gregg, B. A.; Fox, M. A.; Bard, A. J. *J. Phys. Chem.* **1990**, *94*, 1586−1598.
(6) Tang, C. W. *Appl. Phys. Lett.* **1986**, *48*, 183−185.
(7) Wöhrle, D.; Tennigkeit, B.; Elbe, J.; Kreienhoop, L.; Schnurpfeil, G. *Mol. Cryst. Liq. Cryst. A* **1993**, *228*, 221−226.
(8) Wöhrle, D.; Kreienhoop, L.; Schnurpfeil, G.; Elbe, J.; Tennigkeit, B.; Hiller, S.; Schlettwein, D. *J. Mater. Chem.* **1995**, *5*, 1819−1829.
(9) Gregg, B. A. *Chem. Phys. Lett.* **1996**, *258*, 376−380.
(10) Whitlock, J. B.; Panayotatos, P.; Sharma, G. D.; Cox, M. D.; Sauers, R. R.; Birol, G. R. *Opt. Eng.* **1993**, *32*, 1921−1934.
(11) Kamat, P. V.; Chauvet, J.-P.; Fessenden, R. W. *J. Phys. Chem.* **1986**, *90*, 1389−1394.
(12) Kalyanasundaram, K.; Vlachopoulos, N.; Krishnan, V.; Monnier, A.; Grätzel, M. *J. Phys. Chem.* **1987**, *91*, 2342−2347.
(13) Kay, A.; Grätzel, M. *J. Phys. Chem.* **1993**, *97*, 6272−6277.
(14) Kay, A.; Humphry-Baker, R.; Grätzel, M. *J. Phys. Chem.* **1994**, *98*, 952−959.
(15) Boschloo, G. K. Ph.D. Thesis, Technische Universiteit Delft, 1996.
(16) Schlettwein, D.; Armstrong, N. R. *J. Phys. Chem.* **1994**, *98*, 11771−11779.
(17) Yamashita, K.; Harima, Y.; Matsubayashi, T. *J. Phys. Chem.* **1989**, *93*, 5311−5315.
(18) Savenije, T. J.; Koehorst, R. B. M.; Schaafsma, T. J. *Chem. Phys. Lett.* **1995**, *244*, 363−370.
(19) Savenije, T. J.; Moons, E.; Boschloo, G. K.; Goossens, A.; Schaafsma, T. J. *Phys. Rev. B*, in press.
(20) Harima, Y.; Takeda, K.; Yamashita, K. *J. Phys. Chem. Solids* **1995**, *56*, 1223−1229.
(21) Harima, Y.; Kodaka, T.; Okazaki, H.; Kunugi, Y.; Yamashita, K.; Ishii, H.; Seki, K. *Chem. Phys. Lett.* **1995**, *240*, 345−350.
(22) Ishii, H.; Hasegawa, S.; Yoshimura, D.; Sugiyama, K.; Narioka, S.; Sei, M.; Ouchi, Y.; Seki, K.; Harma, Y.; Yamashita, K. *Mol. Cryt. Liq. Cryst.*, in press.
(23) Lüth, H. *Surfaces and Interfaces of Solids*, 2nd ed.; Springer-Verlag: Berlin, 1993.
(24) Jones, R.; Tredgold, R. H.; Hoorfar, A. *Thin Solid Films* **1985**, *123*, 307−314.
(25) Ulman, A. *J. Mater. Educ.* **1989**, *11*, 212−279.
(26) Bruening, M.; Moons, E.; Yaron-Makcovich, D.; Cahen, D.; Libman, J.; Shanzer, A. *J. Am. Chem. Soc.* **1994**, *116*, 2972−2977.
(27) Koenders, L.; Blömacher, M.; Mönch, W. *J. Vac. Sci. Technol.* **1988**, *B6*, 1416−1420.
(28) Nienhaus, H.; Mönch, W. *Appl. Surf. Sci.* **1993**, *65/66*, 632−647.
(29) Bruening, M.; Moons, E.; Cahen, D.; Shanzer, A. *J. Phys. Chem.* **1995**, *99*, 8368−8373.
(30) Moons, E.; Gal, D.; Beier, J.; Hodes, G.; Cahen, D.; Kronik, L.; Burstein, L.; Mishori, B.; Shapira, Y.; Hariskos, D.; Schock, H.-W. *Sol. Energy Mater. Sol. Cells* **1996**, *43*, 73−78.
(31) Kronik, L.; Burstein, L.; Leibovitch, M.; Shapira, Y.; Gal, D.; Moons, E.; Beier, J.; Hodes, G.; Cahen, D.; Hariskos, D.; Klenk, R.; Schock, H.-W. *Appl. Phys. Lett.* **1995**, *67*, 1405−1407.
(32) Kronick, L. Ph.D. Thesis, Tel-Aviv University, 1995.
(33) Armstrong, N. *EMCE96*, private communication, 1996.
(34) Pfeiffer, M.; Leo, K.; Karl, N. *J. Appl. Phys.* **1996**, *80*, 6880.
(35) Hiramoto, M.; Ihara, K.; Fukusumi, H.; Yokoyama, M. *J. Appl. Phys.* **1995**, *78*, 7153−7157.
(36) Marée, T.; Savenije, T. J. *Appl. Surf. Sci.* **1996**, *93*, 291.
(37) Zisman, W. A. *Rev. Sci. Instrum.* **1932**, *3*, 366−371.
(38) Patai, I.; Pomerantz, M. *J. Franklin Inst.* **1951**, 239−260.
(39) Kelvin, L. *Philos. Mag.* **1898**, *46*, 82.
(40) Rossi, F. *Rev. Sci. Instrum.* **1992**, *63*, 4174−4181.
(41) Surplice, N. A.; D'Archy, R. J. *J. Phys. E: Sci. Instrum.* **1970**, *3*, 477−482.
(42) Hamberg, I.; Granqvist, C. G. *J. Appl. Phys.* **1986**, *60*, R123−R159.
(43) Gerfin, T.; Grätzel, M. *J. Appl. Phys.* **1996**, *79*, 1722−1729.
(44) Gerisher, H.; Ekhardt, W. *Appl. Phys. Lett.* **1983**, *43*, 393−395.
(45) Bockris, J. O.; Khan, S. U. M. *Appl. Phys. Lett.* **1984**, *45*, 913.
(46) Reiss, H. *J. Phys. Chem.* **1985**, *89*, 3783−3791.
(47) Kalyanasundaram, K.; Neumann-Spallart, M. *J. Phys. Chem.* **1982**, *86*, 5163−5169.
(48) Urbach *J. Phys. Chem.* **1953**, *92*, 1324.
(49) van den Meerakker, J. E. A. M.; Meulenkamp, E. A.; Scholten, M. *J. Appl. Phys.* **1993**, *74*, 3282−3288.